Journal of Computational Applied Mechanics 2022, 53(2): 169-182

DOI: 10.22059/JCAMECH.2022.341592.711

RESEARCH PAPER

Routing and avoiding collisions of autonomous robots in unknown environments with fixed and moving obstacles

Alireza Makvandi, Hesam Makvandi*

Department of Engineering, Abadan Branch, Islamic Azad University, Abadan, Iran

Abstract

This research employs a hierarchical fuzzy control method to guide and control autonomous robots in environments containing fixed and moving obstacles. Considering that robots must operate in social environments to serve humans better, they must be able to navigate in the presence of fixed obstacles, moving objects and people without colliding or creating a fear of collision, and reach the final destination. The current work utilizes a hierarchical fuzzy controller with three agents of navigation, obstacle avoidance, and perception to achieve these goals. The coordination between these three agents is done using the definition of special utility functions. The obtained results confirm the correctness of the proposed approach in the successful passage of the robot past the fixed and moving obstacles and bringing it to the target point.

Keywords: Autonomous Robots, Navigation, Avoiding Obstacles, Hierarchical Fuzzy Control, Type-II Fuzzy Logic Controller.

1. Introduction

The obtained route for the robot to reach the desired destination is highly dependent on the employed approaches. The optimality of the chosen path, a function of the conditions and limitations of the robot and the path itself, is crucial here. Time is of the essence in many applications of the robot. For example, in rescue robots, people's lives depend on the correct and optimal operation of the robot routing system and the timely arrival of the robot to the injured. There are many different methods for routing autonomous robots in the articles, and the number of these methods is increasing every day. Therefore, choosing the right approach to meet the constraints is challenging.

Using fuzzy logic, Nasrinahar and Chuah [1] presented a method to effectively guide the robot through fixed and moving obstacles with various geometric shapes and movements. Their robot was equipped with nine sensors to detect the distance and direction of the obstacle to the robot. Innocenti et al. [1] presented a multi-agent system to guide the robot using four subsystems. They used fuzzy sets to model the relationship between different controllers. The use of multi-agent systems has been observed in other cases as well. Ono et al. [2] proposed a multi-agent system to control a wheelchair. They considered four agents: sensor controller, corridor detector, collision avoidance, and locomotion agent.

Mehrez et al. [3] used an optimization-based method to control a relative localization and a relative tracking control in multi-robot systems. In this method, one or more robots are placed in one place and are guided in different directions according to the reference robot. MohammadrezaeiNodeh et al. [4] combined fuzzy logic with neural network and high-order sliding mode to control a robotic arm under significant and uncertain parametric disturbance. They observed that the proposed approach is more durable than the classic sliding mode in the presence

* Hesam Makvandi. Tel.: +989163206247; fax: +986134412547.
E-mail address: h.makvandi@iauabadan.ac.ir

of uncertainty and disturbance and can adequately handle the robotic arm under the desired conditions. Tanha et al. [5] used the fuzzy control method to guide the robot in the presence of fixed and moving obstacles. Tikni and Shahbazi [6] controlled the angular position on a quadrator using fuzzy control algorithm and Kalman filter. They used a Kalman filter to remove noise from the sensor output. Ghanavati et al. [7] used a proportional-integral-derivative fuzzy controller to control a 2D cable robot. They used the Krill Herd optimization algorithm to determine the coefficients of the controllers and succeeded in maintaining the tensile force of the cables while quickly guiding the robot. Woong-Gie et al. [8] used genetic algorithm to achieve the shortest path in environments with moving obstacles. Many other researchers have used evolutionary algorithms in this field, such as Mac et al. [9], Che et al. [10], Luo et al. [11] ,who used PSO ,gray wolf, and ACO algorithms, respectively, to route the robot.

One common type of fuzzy systems that has attracted the attention of many researchers in the field of modelling and design of these systems is the so-called hierarchical fuzzy system [12, 13].These systems consist of a fuzzy structure composed of several smaller fuzzy subsystems that are hierarchically arranged. These hierarchical fuzzy subsystems make it possible to reduce the number of fuzzy rules compared to a standard fuzzy system [14]. Feng et al. [15] have used deep reinforcement learning to solve collision avoidance problems in an unknown environment, especially in narrow corridors. Their experimental results shown that the proposed approach was able to perform well in previously unseen scenarios that are much different from the training scenario, thereby proving a generalized nature of the trained architecture. Krell et al. [16] have used Particle Swarm Optimization (PSO) to develop an autonomous robot navigation system that can navigate in an unknown environment, reaching a pre-defined goal and become collision-free. They have found that PSO has high performance in searching for the optimal path. There are many other related articles in similar fields that can be considered [17-52].

A variety of methods have been proposed to guide autonomous robots. Many of the approaches presented so far have some limitations. Since the robot must provide services to humans, developing methods to route them in social environments is necessary. The movement of the robot to the target point in such settings should be without causing a fear response in humans. This research aims to control the robot using a multi-agent system to achieve the desired position without colliding fixed and moving obstacles. For this purpose, first, the two behaviours, i.e., reaching the position and avoiding collision with obstacles, will be modelled using two agents. The robot navigation agent is a simple fuzzy control. Nevertheless, to avoid collisions, the information sent by the eight sensors installed on the robot is used to determine the location of obstacles. Due to the large number of input variables and fuzzy rules and the resulting implementation problems of such a controller, a hierarchical fuzzy controller has been employed to develop this agent. Moreover, the type-II fuzzy set has been used as fuzzy controllers to reduce the effect of system uncertainties. In what follows, after introducing the intended kinematics of the robot, the hierarchical fuzzy control method and the obtained results are presented.

2. Robot kinematic

In this section, the structure of the desired wheeled robot will be explained, and the governing dynamic equations will be presented. For this purpose, a robot such as the one depicted in Figure (1),a non-holonomic mobile robot with two wheels that move independently, is considered. To steer the robot, it is necessary to control the speed of the wheels. Therefore, the motion model of the robot is considered as Equation (1):

$$\begin{cases} \dfrac{dX_R}{dt} = \dfrac{V_R + V_L}{2}\cos\alpha_R \\ \dfrac{dY_R}{dt} = \dfrac{V_R + V_L}{2}\sin\alpha_R \\ \dfrac{d\alpha_R}{dt} = \dfrac{V_R - V_L}{L} \end{cases} \tag{1}$$

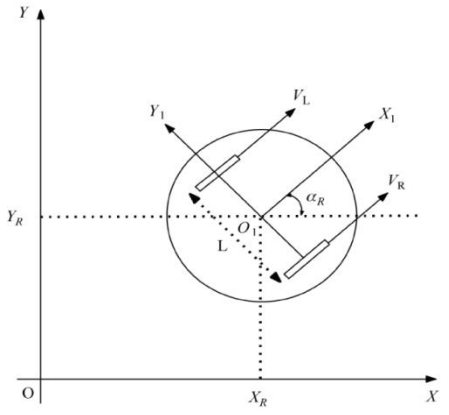

Figure 1: Schematic model of a mobile robot

X_R and Y_R are the coordinates of the robot's center of gravity on the plane. Where V_R and V_L denote the speeds of the right and left wheels, respectively, α_R is the angle of the robot relative to the X axes, and L is the distance between the two wheels of the robot.

3. Robot control structure

The proposed structure for robot control is presented in Figure (2).This structure has three agents: perception agent, robot navigation agent, and obstacle avoidance agent. These agents can communicate with each other to coordinate and ensure the correct behavior of the whole set.

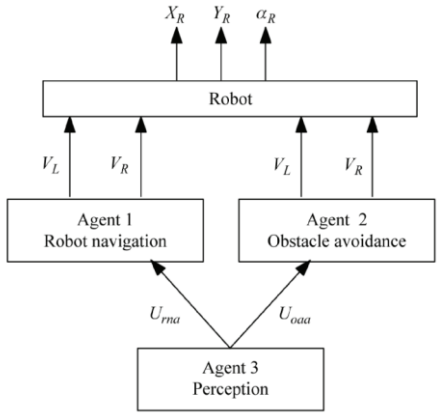

Figure 2: Proposed structure for robot control

4. Robot navigation agent

In this section, an obstacle-free environment is assumed. The robot must find a way to reach the target position. The fuzzy controller has inputs d (indicating the distance from the centre of the robot to the position of the target) and φ (indicating the angle between the robot and the target), as shown in Figure (3).The parameters d and φ are calculated using Equations (2) and (3), respectively:

$$d = \sqrt{(X_T - X_R)^2 + (Y_T - Y_R)^2} \tag{2}$$

$$\varphi = \theta_T - \alpha_R \tag{3}$$

$$\theta_T = \arctan\frac{Y_T - Y_R}{X_T - X_R} \tag{4}$$

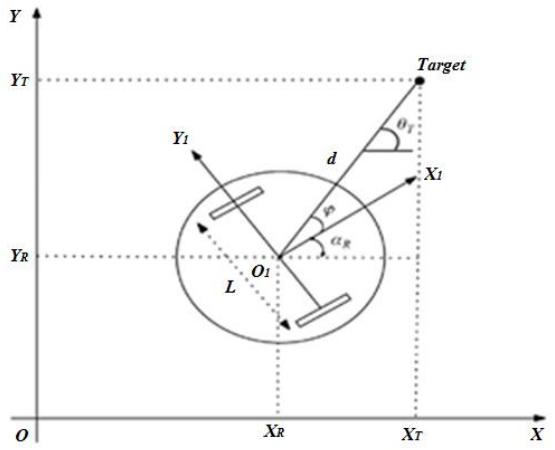

Figure 3: Angle between robot and target

Where X_T and Y_T are the coordinates of target point. Unlike binary variables (which are either true or false), fuzzy variables offer a wide range of variations of input variables. The distance d is considered to be between 0 and 700 mm, while the angle φ is defined in the range [15].The membership functions of parameters d and φ are defined in Gaussian form as in Equation (5).

$$Gauss(x,\sigma,a)=\exp\left[-\left(\frac{x-a}{\sigma}\right)^2\right] \tag{5}$$

Here are five fuzzy membership functions (VS: very small, S: small, M: medium, L: large, VL: very large) for the distance d and seven membership functions (NL: negative large, NM: negative medium, NS: negative Small, Z: zero, PS: positive small, PM: positive medium, PL: positive large) for the angle φ leads to desirable results. Therefore, this controller has only 35 fuzzy rules. The proposed fuzzy rules for right wheel and left wheel speeds are shown in Figures (4) and (5), respectively. The output of the fuzzy speed controller is the speed of the left and right wheels (V_L and V_R).

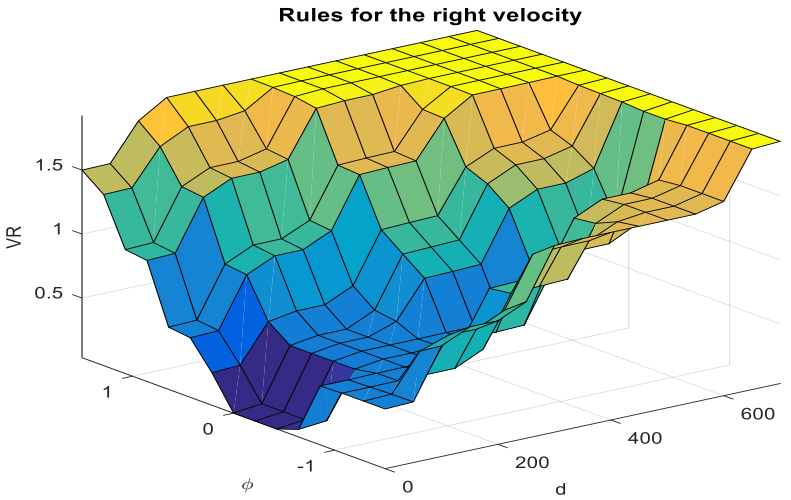

Figure 4: Three-dimensional presentation of fuzzy rules related to right wheel speed.

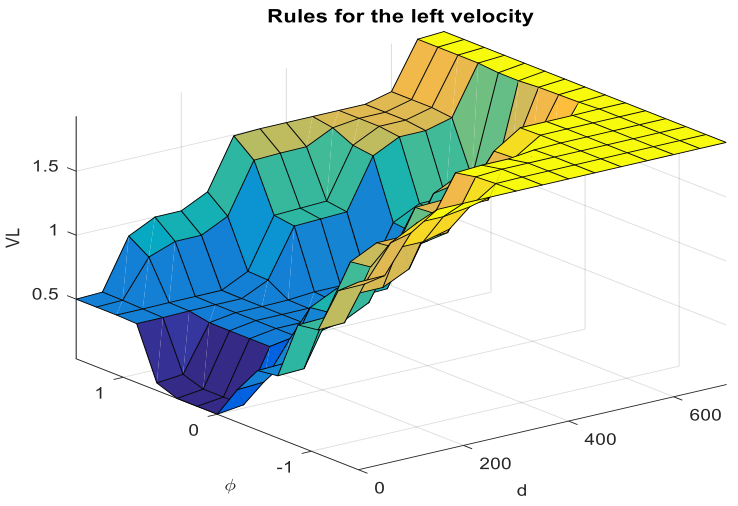

Figure 5: Three-dimensional presentation of fuzzy rules related to left wheel speed.

5. Obstacle avoidance agent

In this section, the robot is guided by considering obstacles. To ensure the safety of the robot and humans, the robot must avoid collisions with obstacles. Eight sensors are used on the robot to detect obstacles, as shown in Figure (6).

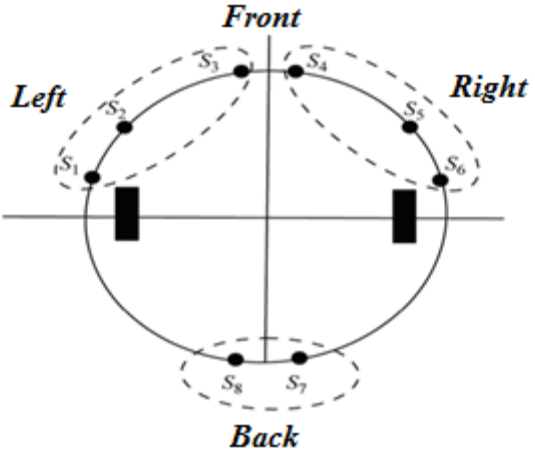

Figure 6: Position of eight sensors on the robot.

The angle of the robot with respect to the horizontal axis X is considered zero. Consequently, the sensors are mounted on the robot with the following angles:

$$S_1 = 70^\circ \quad , S_2 = 50^\circ \quad , S_3 = 10^\circ ,$$
$$S_4 = -10^\circ \quad , S_5 = -50^\circ , S_6 = -70^\circ , \tag{6}$$
$$S_7 = -170^\circ , S_8 = 170^\circ$$

Each sensor provides the distance d_i and the angle φ_i between the robot and the obstacle (i = 1,2,…, 8). If only one fuzzy controller is used to avoid obstacles, all angles and distances between possible combinations provided by the eight sensors must be considered. In this case, if five membership functions for each distance and seven membership functions for each angle are considered, the number of fuzzy rules will be equal to $7^8 \times 5^8$, which

is very difficult and almost impossible to consider. An approach based on hierarchical fuzzy systems similar to Figure (7) is used to solve this problem.

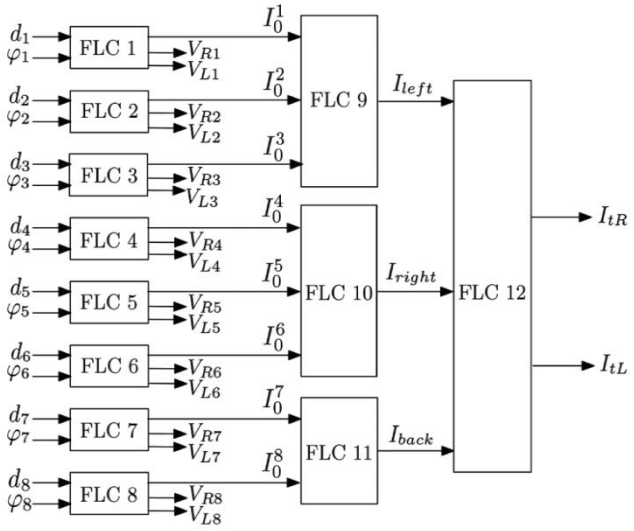

Figure 7: Hierarchical fuzzy system diagram block.

The output of these controllers is an index I_0^i, which indicates the degree to which the robot encounters an obstacle. Table (1) presents the rules related to the index I_0^i. 0 refers to the distance away from the robot, 1 refers to the relative proximity of the obstacle to the robot, and 2 refers to the proximity of the obstacle to the robot.

Table 1: Fuzzy rules for the index I_0^i.

		φ_i						
I_0^i		*NL*	*NM*	*NS*	*Z*	*PS*	*PM*	*PL*
d_i	*VS*	*2*	*2*	*2*	*2*	*2*	*2*	*2*
	S	*1*	*2*	*2*	*2*	*2*	*2*	*1*
	M	*0*	*1*	*1*	*1*	*1*	*1*	*0*
	L	*0*	*0*	*0*	*1*	*0*	*0*	*0*
	VL	*0*	*0*	*0*	*0*	*0*	*0*	*0*

In Figure (7), sensors S_1, S_2, S_3 are installed to detect obstacles on the left side of the robot, and sensors S_4, S_5, S_6 on the right side, and S_8, S_7 behind the robot. Moreover, for communication of each sensor group, a fuzzy controller, as shown in Figure (7), is used to detect local obstacles around the robot. Therefore, through the FLC9, FLC10, and FLC11 controllers, the I_{right}, I_{left} and I_{back} indices are obtained, which indicate the degree of collision between the robot and the obstacle on the left, right and back, respectively. An additional controller will be added at this level, responsible for maintaining direction with the goal and avoiding obstacles. This controller provides the degree of absence of obstacles by two output indicators I_{tR} and I_{tL}, so that according to it, the robot can find the direction of the target. The rules for I_{tR} and I_{tL} outputs are shown in Tables (2) and (3), three numerical values are used as indicators. In this case, a value of zero indicates the proximity of the obstacle to the robot. Therefore, the robot must change its direction of movement. A value of 5 indicates that the obstacle is relatively close to the robot, in which case the robot can move at a slow speed and at the same time correct its direction of movement. When there are no obstacles around the robot, a value of 10 will be used, in which case the robot can continue to advance without any problems.

Table 2: Discrete values for the I_{tL} index.

I_{tL}		I_{left}								
		Z			*M*			*L*		
		I_{right}			I_{right}			I_{right}		
		Z	*M*	*L*	*Z*	*M*	*L*	*Z*	*M*	*L*
I_{back}	*Z*	*10*	*5*	*0*	*10*	*10*	*0*	*10*	*10*	*0*
	M	*10*	*5*	*0*	*10*	*10*	*0*	*10*	*10*	*0*
	L	*10*	*5*	*0*	*10*	*5*	*0*	*10*	*10*	*0*

Table 3: Discrete values for the I_{tR} index.

I_{tL}		I_{left}								
		Z			*M*			*L*		
		I_{right}			I_{right}			I_{right}		
		Z	*M*	*L*	*Z*	*M*	*L*	*Z*	*M*	L
I_{back}	*Z*	*10*	*10*	*10*	*5*	*5*	*10*	*0*	*0*	1 0
	M	*10*	*10*	*10*	*5*	*5*	*10*	*0*	*0*	1 0
	L	*10*	*10*	*10*	*5*	*10*	*10*	*0*	*0*	1 0

6. Utility function

Since the navigation agent and the obstacle avoidance agent can exhibit conflicting behaviours, a utility function whose value is defined in the range [15] is proposed to resolve this conflict. This function will allow negotiation between the robot control agents. First, the usefulness of the robot navigation agent is calculated as a function of the distance remaining to the target. On the other hand, the obstacle avoidance agent is calculated as a utility function depending on the distance from the distance to the obstacle and the angle between the direction of the robot and the obstacle. The utility functions used in this research are shown in Figure (8).

7. Results

7.1. Environment without obstacles

Ac This section aims to evaluate the efficiency of the robot navigation agent to achieve the desired position. Therefore, there is no obstacle in the robot's movement environment in this scenario, and the robot can move freely in all directions to reach the target location. Here the robot is in the initial position at the beginning of the movement $(X_R, Y_R) = (0,0)$ and the goal is for the robot to reach the place $(X_T, Y_T) = (500,300)$. It should be noted that the distance between the two wheels of the robot is equal to L = 80mm. Figure (9) shows the path taken by the robot to reach the target position. As can be clearly seen in this figure, by using the proposed navigation algorithm, the robot was able to reach the desired location and stay there.

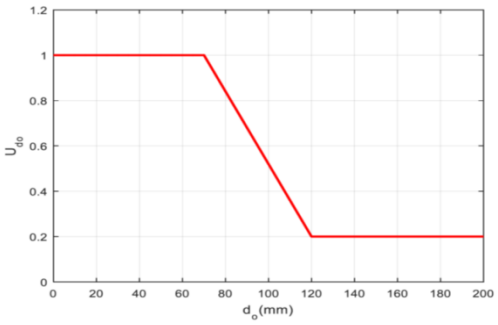

(b)

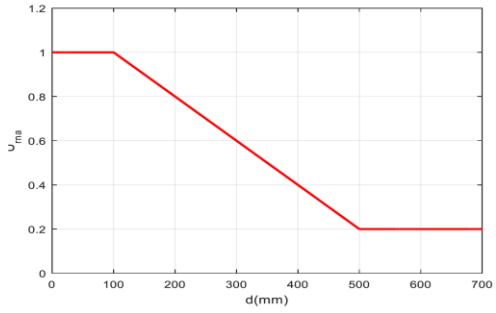

(a)

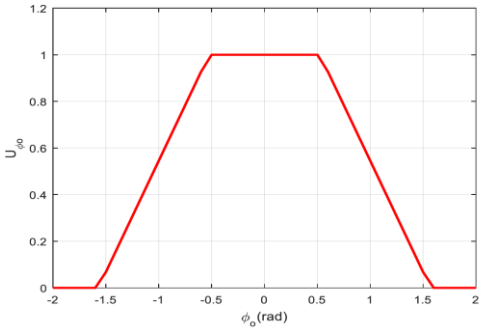

(c)

Figure 8: (a) utility function of robot navigation agent (b) Utility function of distance-dependent obstacle avoidance agent (c) Function of angle-dependent obstacle avoidance agent.

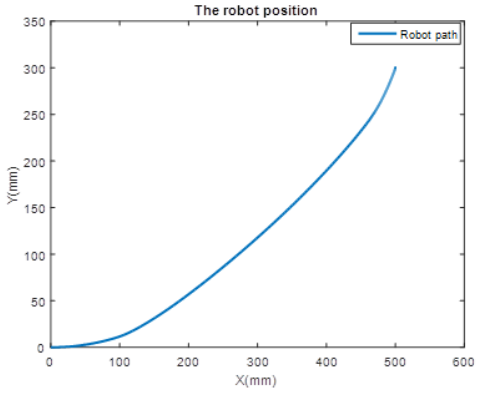

Figure 9: The path taken by the center of the robot.

Figure (10) shows the speed of the robot's right and left wheels. As can be seen in this figure, at the beginning of the movement, the speed range of the robot is high and with the passage of time and closer to the target location, the speed decreases and when the robot reaches the target position, it tends to zero. This confirms the correctness of the proposed navigation agent, because at the beginning of the movement, due to the distance of the robot from the desired location, the robot must increase its speed in order to reach the desired location as quickly as possible. Following the path and approaching the target location, the accuracy of achieving the desired location and staying in that location becomes important, therefore, the robot must reduce its speed so that after reaching the desired location, its speed should be zero.

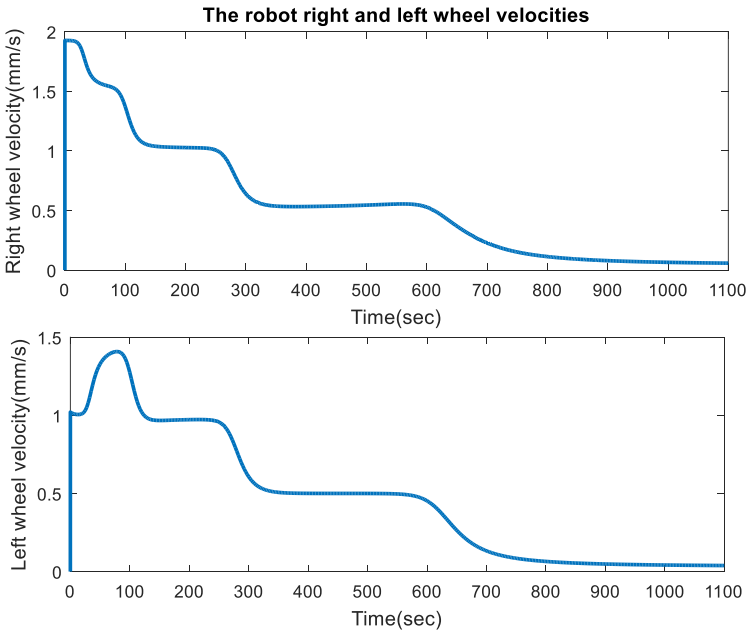

Figure 10: Robot right and left wheel speeds.

Figure (11) shows how the robot navigation and obstacle avoidance agents are activated. A value of one indicates the activation of the relevant agent, and the number zero indicates the inactivity of the agent .As can be seen in this figure, the robot navigation agent is active along the entire path, and the obstacle avoidance agent remains inactive throughout the path. This result indicates the successful operation of the utility function. Because, in the scenario defined in this section, there is no obstacle to activate the obstacle avoidance agent.

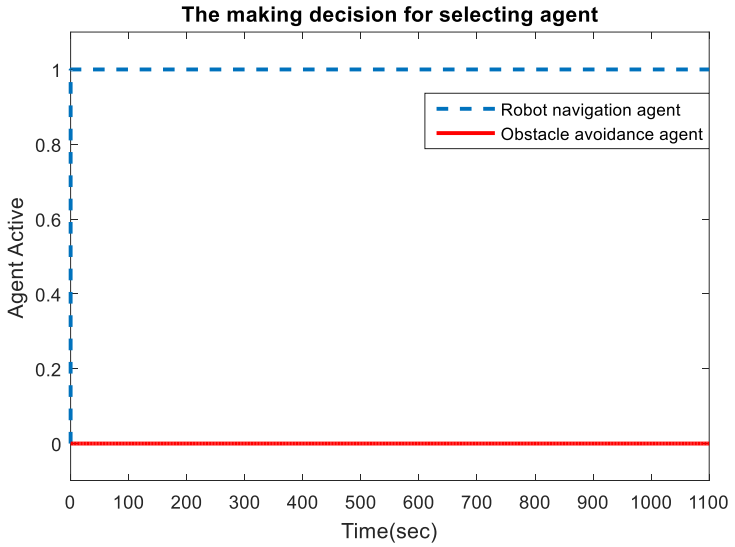

Figure 11: operation of robot navigation and avoid obstacles agents.

7.2. Obstacles in the path of the robot

The purpose of this section is to show the successful performance of the proposed multi-agent control algorithm in the face of obstacles on both sides of the robot to achieve the desired position and avoid obstacles. Therefore, consider three circular obstacles in coordinates (X_{o1}, Y_{o1}) = (120, -10) and (X_{o2}, Y_{o2}) = (100,300) and (X_{o3}, Y_{o3}) = (500,300) each with radius d_o = 50mm get. The second obstacle is moving the line directly to the point

(0,500).Also, the robot is in the initial position at the beginning of the movement (X_R, Y_R) = (0,0), and the goal of the robot is to reach the place (X_T, Y_T) = (600,500).

Figure (12) shows the path taken by the robot to reach the target position in the presence of obstacles. As can be clearly seen in this figure, by using the proposed multi-agent control algorithm, the robot was able to reach the desired location and stay in the same place without colliding obstacles and maintaining a suitable distance from them.

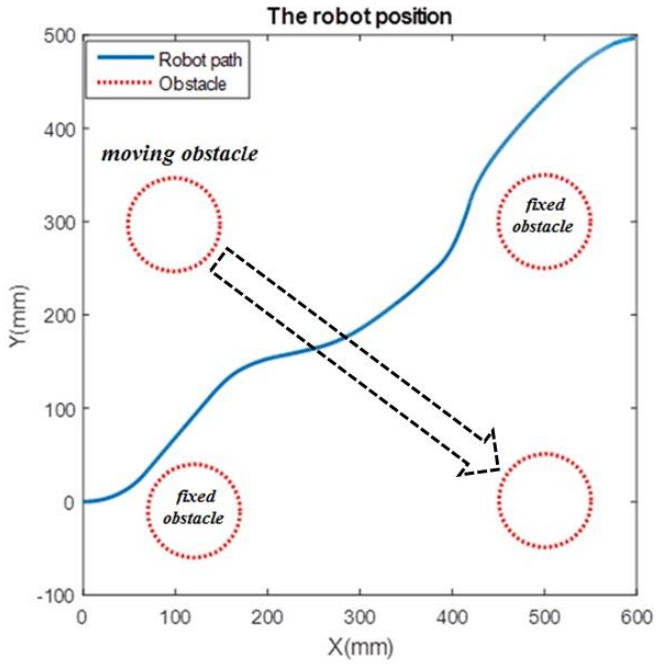

Figure 12: The path taken by the center of the robot in the presence of three obstacles on both sides to reach the desired location.

Figure (13) shows the speed of the right and left wheels of the robot in the presence of obstacles. As can be seen in this figure, at the beginning of the movement, the robot's right wheel speed range is faster than the left wheel speed in order to bypass the first obstacle from the right. In the continuation of the route, the speed range of the left wheel of the robot in order to bypass the second obstacle from the left, increases the speed of the right wheel, and passes the third obstacle as the first obstacle. After that, by crossing the obstacles, the robot navigation agent takes control of the robot speed from 180th onwards, and the speed of both wheels is reduced to reach the target position more accurately.

Figure (14) shows how the robot navigation and obstacle avoidance agents are activated. As can be seen in this figure, at the beginning of the movement, due to the presence of an obstacle and also the distance of the robot from the desired position, the avoidance agent is responsible for guiding the robot until the 10th second, then by passing the first obstacle, the robot navigation agent approaches Activated on the second obstacle (up to the 50th second).As robot approach the second obstacle, the obstacle avoidance agent is activated once again in the 50th second and remains active until the 100th second. The obstacle avoidance agent will be deactivated by crossing the second obstacle, and the robot navigation agent will be activated until reaching the third obstacle. As we approach the third obstacle, the obstacle avoidance agent is activated once again in the 150th second and remains active until the 180th second. After crossing the third obstacle, the navigation agent is activated to the end of the route. This result indicates the successful operation of the utility function and the full coordination of agents with each other.

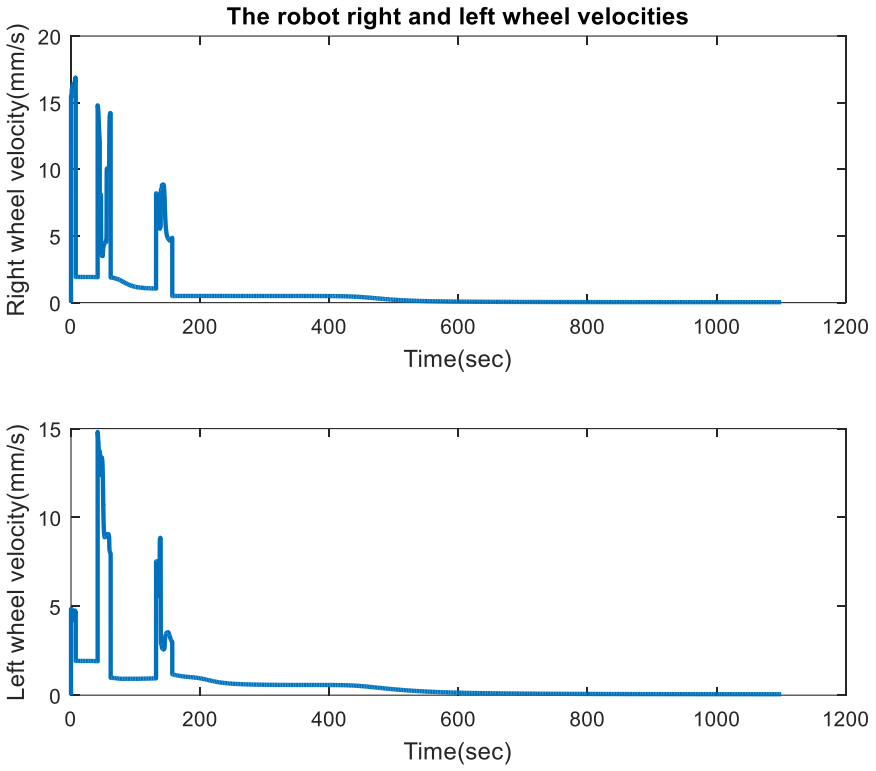

Figure 13: The speed of the right and left wheels of the robot in the presence of three obstacles on both sides.

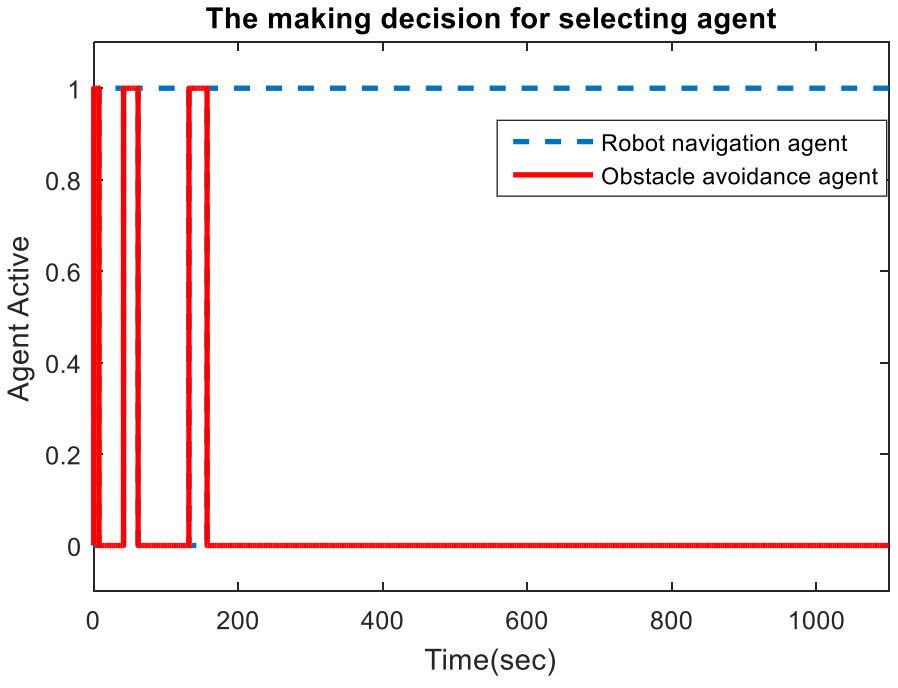

Figure 14: operation of the robot navigation and avoiding obstacle agents in the presence of three obstacles on both sides.

8. Conclusion

This study aimed to develop an approach to navigate the robot in unknown environments. The robot should be able to reach the target without colliding obstacles. For this purpose, a method based on the multi-operating system model was proposed. In this controller, three agents were considered: the first agent using the fuzzy controller to ensure that the robot reached the desired location. The second agent uses a hierarchical fuzzy controller to prevent the robot from colliding obstacles in the path. This hierarchical controller reduced the number of fuzzy rules according to the number of fuzzy input variables. Finally, the third or perception agent was responsible for collecting and presenting information about the robot's environment. The proposed method to coordinate and eliminate the conflict between the agents in this study was to use a utility function. The simulation results showed the successful performance of the proposed controller so that the robot was able to reach the target position in an environment with various obstacles without colliding them.

References

[1] B. Innocenti, B. López, J. Salvi, A multi-agent architecture with cooperative fuzzy control for a mobile robot, *Robotics and Autonomous Systems*, Vol. 55, No. 12, pp. 881-891, 2007.

[2] Y. Ono, H. Uchiyama, W. Potter, 2004, *A mobile robot for corridor navigation: A multi-agent approach*,

[3] M. W. Mehrez, G. K. I Mann, R. G. Gosine, An optimization based approach for relative localization and relative tracking control in multi-robot systems, *Journal of Intelligent & Robotic Systems*, Vol. 85, No. 2, pp. 385-408, 2017.

[4] S. Mohammadrezaei Nodeh, M. H. Ghasemi, H. R. Mohammadi Daniali, Hybrid Control of Fuzzy Type 2-Neural Network and Higher Order Sliding Mode for Robotic Manipulator with Parametric Uncertainties and Perturbations, *Journal of Mechanical Engineering*, Vol. 51, No. 1, pp. 219-228, 2021.

[5] s. d. nikkhoe tanha, M. Habibnejad korayem, s. fathollahi dehkordi, Path Design and Control of a Moving Social Robot in an Environment with Moving Obstacles in Order to Reach a Moving Target through Fuzzy Control, *Amirkabir Journal of Mechanical Engineering*, Vol. 53, No. 2, pp. 993-1014, 2021.

[6] V. Tikani, h. S. Shahbazi, Design and Implementation of Pure Fuzzy Controller for Attitude Control of Quadrotor using Kalman Filter, *Journal of Mechanical Engineering*, Vol. 48, No. 2, pp. 65-73, 2018.

[7] A. Ghanavati, M. J. Mahmoodabadi, M. Beigzadeh Abbasi, Optimal Design of the Proportional-Integral-Derivative Fuzzy Controller for a Three Degree-of-Freedom Plane Cable Robot based on Krill Herd Optimization, *Journal of Mechanical Engineering*, Vol. 51, No. 1, pp. 183-192, 2021.

[8] H. Woong-Gie, B. Seung-Min, K. Tae-Yong, Genetic algorithm based path planning and dynamic obstacle avoidance of mobile robots, in *Proceeding of*, 2747-2751 vol.3.

[9] T. T. Mac, C. Copot, D. T. Tran, R. De Keyser, A hierarchical global path planning approach for mobile robots based on multi-objective particle swarm optimization, *Applied Soft Computing*, Vol. 59, pp. 68-76, 2017.

[10] H. Che, Z. Wu, R. Kang, C. Yun, Global path planning for explosion-proof robot based on improved ant colony optimization, in *Proceeding of*, IEEE, pp. 36-40.

[11] Q. Luo, H. Wang, Y. Zheng, J. He, Research on path planning of mobile robot based on improved ant colony algorithm, *Neural Computing and Applications*, Vol. 32, No. 6, pp. 1555-1566, 2020.

[12] G. Raju, J. Zhou, R. A. Kisner, Hierarchical fuzzy control, *International journal of control*, Vol. 54, No. 5, pp. 1201-1216, 1991.

[13] M. G. Joo, J. S. Lee, Hierarchical fuzzy control scheme using structured Takagi-Sugeno type fuzzy inference, in *Proceeding of*, IEEE, pp. 78-83.

[14] M.-L. Lee, H.-Y. Chung, F.-M. Yu, Modeling of hierarchical fuzzy systems, *Fuzzy sets and systems*, Vol. 138, No. 2, pp. 343-361, 2003.

[15] S. Feng, B. Sebastian, P. Ben-Tzvi, A Collision Avoidance Method Based on Deep Reinforcement Learning, *Robotics*, Vol. 10, No. 2, pp. 73, 2021.

[16] E. Krell, A. Sheta, A. P. R. Balasubramanian, S. A. King, Collision-Free Autonomous Robot Navigation in Unknown Environments Utilizing PSO for Path Planning, *Journal of Artificial Intelligence and Soft Computing Research*, Vol. 9, No. 4, pp. 267-282, 2019.

[17] M. Mohammadi, M. Ghayour, A. Farajpour, Analysis of free vibration sector plate based on elastic medium by using new version of differential quadrature method, *Journal of Simulation and Analysis of Novel Technologies in Mechanical Engineering,* Vol. 3, No. 2, pp. 47-56, 2010.

[18] A. Farajpour, M. Danesh, M. Mohammadi, Buckling analysis of variable thickness nanoplates using nonlocal continuum mechanics, *Physica E: Low-dimensional Systems and Nanostructures,* Vol. 44, No. 3, pp. 719-727, 2011.

[19] A. Farajpour, M. Mohammadi, A. Shahidi, M. Mahzoon, Axisymmetric buckling of the circular graphene sheets with the nonlocal continuum plate model, *Physica E: Low-dimensional Systems and Nanostructures,* Vol. 43, No. 10, pp. 1820-1825, 2011.

[20] N. Ghayour, A. Sedaghat, M. Mohammadi, Wave propagation approach to fluid filled submerged visco-elastic finite cylindrical shells, 2011.

[21] H. Moosavi, M. Mohammadi, A. Farajpour, S. Shahidi, Vibration analysis of nanorings using nonlocal continuum mechanics and shear deformable ring theory, *Physica E: Low-dimensional Systems and Nanostructures,* Vol. 44, No. 1, pp. 135-140, 2011.

[22] A. Farajpour, M. Mohammadi, A. R. Shahidi, M. Mahzoon, Axisymmetric buckling of the circular graphene sheets with the nonlocal continuum plate model, *Physica E: Low-dimensional Systems and Nanostructures,* Vol. 43, No. 10, pp. 1820-1825, 2011/08/01/, 2011.

[23] M. Mohammadi, M. Ghayour, A. Farajpour, ANALYSIS OF FREE VIBRATION SECTOR PLATE BASED ON ELASTIC MEDIUM BY USING NEW VERSION OF DIFFERENTIAL QUADRATURE METHOD, *JOURNAL OF SIMULATION AND ANALYSIS OF NOVEL TECHNOLOGIES IN MECHANICAL ENGINEERING (JOURNAL OF SOLID MECHANICS IN ENGINEERING),* Vol. 3, No. 2, pp. 47-56, 2011. English

[24] M. Danesh, A. Farajpour, M. Mohammadi, Axial vibration analysis of a tapered nanorod based on nonlocal elasticity theory and differential quadrature method, *Mechanics Research Communications,* Vol. 39, No. 1, pp. 23-27, 2012.

[25] A. Farajpour, A. Shahidi, M. Mohammadi, M. Mahzoon, Buckling of orthotropic micro/nanoscale plates under linearly varying in-plane load via nonlocal continuum mechanics, *Composite Structures,* Vol. 94, No. 5, pp. 1605-1615, 2012.

[26] M. Mohammadi, M. Goodarzi, M. Ghayour, S. Alivand, Small scale effect on the vibration of orthotropic plates embedded in an elastic medium and under biaxial in-plane pre-load via nonlocal elasticity theory, 2012.

[27] M. Mohammadi, A. Farajpour, M. Goodarzi, R. Heydarshenas, Levy type solution for nonlocal thermo-mechanical vibration of orthotropic mono-layer graphene sheet embedded in an elastic medium, *Journal of Solid Mechanics,* Vol. 5, No. 2, pp. 116-132, 2013.

[28] M. Mohammadi, A. Farajpour, M. Goodarzi, H. Mohammadi, Temperature Effect on Vibration Analysis of Annular Graphene Sheet Embedded on Visco-Pasternak Foundati, *Journal of Solid Mechanics,* Vol. 5, No. 3, pp. 305-323, 2013.

[29] M. Mohammadi, M. Ghayour, A. Farajpour, Free transverse vibration analysis of circular and annular graphene sheets with various boundary conditions using the nonlocal continuum plate model, *Composites Part B: Engineering,* Vol. 45, No. 1, pp. 32-42, 2013.

[30] M. Mohammadi, M. Goodarzi, M. Ghayour, A. Farajpour, Influence of in-plane pre-load on the vibration frequency of circular graphene sheet via nonlocal continuum theory, *Composites Part B: Engineering,* Vol. 51, pp. 121-129, 2013.

[31] S. Asemi, A. Farajpour, H. Asemi, M. Mohammadi, Influence of initial stress on the vibration of double-piezoelectric-nanoplate systems with various boundary conditions using DQM, *Physica E: Low-dimensional Systems and Nanostructures,* Vol. 63, pp. 169-179, 2014.

[32] S. Asemi, A. Farajpour, M. Mohammadi, Nonlinear vibration analysis of piezoelectric nanoelectromechanical resonators based on nonlocal elasticity theory, *Composite Structures,* Vol. 116, pp. 703-712, 2014.

[33] S. R. Asemi, M. Mohammadi, A. Farajpour, A study on the nonlinear stability of orthotropic single-layered graphene sheet based on nonlocal elasticity theory, *Latin American Journal of Solids and Structures,* Vol. 11, No. 9, pp. 1515-1540, 2014.

[34] A. Farajpour, A. Rastgoo, M. Mohammadi, Surface effects on the mechanical characteristics of microtubule networks in living cells, *Mechanics Research Communications,* Vol. 57, pp. 18-26, 2014.

[35] M. Goodarzi, M. Mohammadi, A. Farajpour, M. Khooran, Investigation of the effect of pre-stressed on vibration frequency of rectangular nanoplate based on a visco-Pasternak foundation, 2014.

[36] M. Mohammadi, A. Farajpour, M. Goodarzi, F. Dinari, Thermo-mechanical vibration analysis of annular and circular graphene sheet embedded in an elastic medium, *Latin American Journal of Solids and Structures,* Vol. 11, pp. 659-682, 2014.

[37] M. Mohammadi, A. Farajpour, M. Goodarzi, Numerical study of the effect of shear in-plane load on the vibration analysis of graphene sheet embedded in an elastic medium, *Computational Materials Science,* Vol. 82, pp. 510-520, 2014.

[38] M. Mohammadi, A. Farajpour, A. Moradi, M. Ghayour, Shear buckling of orthotropic rectangular graphene sheet embedded in an elastic medium in thermal environment, *Composites Part B: Engineering,* Vol. 56, pp. 629-637, 2014.

[39] M. Mohammadi, A. Moradi, M. Ghayour, A. Farajpour, Exact solution for thermo-mechanical vibration of orthotropic mono-layer graphene sheet embedded in an elastic medium, *Latin American Journal of Solids and Structures,* Vol. 11, No. 3, pp. 437-458, 2014.

[40] H. Asemi, S. Asemi, A. Farajpour, M. Mohammadi, Nanoscale mass detection based on vibrating piezoelectric ultrathin films under thermo-electro-mechanical loads, *Physica E: Low-dimensional Systems and Nanostructures,* Vol. 68, pp. 112-122, 2015.

[41] M. Safarabadi, M. Mohammadi, A. Farajpour, M. Goodarzi, Effect of surface energy on the vibration analysis of rotating nanobeam, 2015.

[42] H. R. Asemi, S. R. Asemi, A. Farajpour, M. Mohammadi, Nanoscale mass detection based on vibrating piezoelectric ultrathin films under thermo-electro-mechanical loads, *Physica E: Low-dimensional Systems and Nanostructures,* Vol. 68, pp. 112-122, 2015/04/01/, 2015.

[43] M. Baghani, M. Mohammadi, A. Farajpour, Dynamic and stability analysis of the rotating nanobeam in a nonuniform magnetic field considering the surface energy, *International Journal of Applied Mechanics,* Vol. 8, No. 04, pp. 1650048, 2016.

[44] A. Farajpour, M. H. Yazdi, A. Rastgoo, M. Loghmani, M. Mohammadi, Nonlocal nonlinear plate model for large amplitude vibration of magneto-electro-elastic nanoplates, *Composite Structures,* Vol. 140, pp. 323-336, 2016.

[45] A. Farajpour, M. Yazdi, A. Rastgoo, M. Mohammadi, A higher-order nonlocal strain gradient plate model for buckling of orthotropic nanoplates in thermal environment, *Acta Mechanica,* Vol. 227, No. 7, pp. 1849-1867, 2016.

[46] M. R. Farajpour, A. Rastgoo, A. Farajpour, M. Mohammadi, Vibration of piezoelectric nanofilm-based electromechanical sensors via higher-order non-local strain gradient theory, *Micro & Nano Letters,* Vol. 11, No. 6, pp. 302-307, 2016.

[47] M. Mohammadi, M. Safarabadi, A. Rastgoo, A. Farajpour, Hygro-mechanical vibration analysis of a rotating viscoelastic nanobeam embedded in a visco-Pasternak elastic medium and in a nonlinear thermal environment, *Acta Mechanica,* Vol. 227, No. 8, pp. 2207-2232, 2016.

[48] M. Goodarzi, M. Mohammadi, M. Khooran, F. Saadi, Thermo-mechanical vibration analysis of FG circular and annular nanoplate based on the visco-pasternak foundation, *Journal of Solid Mechanics,* Vol. 8, No. 4, pp. 788-805, 2016.

[49] A. Farajpour, A. Rastgoo, M. Mohammadi, Vibration, buckling and smart control of microtubules using piezoelectric nanoshells under electric voltage in thermal environment, *Physica B: Condensed Matter,* Vol. 509, pp. 100-114, 2017.

[50] M. Mohammadi, M. Hosseini, M. Shishesaz, A. Hadi, A. Rastgoo, Primary and secondary resonance analysis of porous functionally graded nanobeam resting on a nonlinear foundation subjected to mechanical and electrical loads, *European Journal of Mechanics-A/Solids,* Vol. 77, pp. 103793, 2019.

[51] M. Mohammadi, A. Rastgoo, Nonlinear vibration analysis of the viscoelastic composite nanoplate with three directionally imperfect porous FG core, *Structural Engineering and Mechanics, An Int'l Journal,* Vol. 69, No. 2, pp. 131-143, 2019.

[52] M. Mohammadi, A. Rastgoo, Primary and secondary resonance analysis of FG/lipid nanoplate with considering porosity distribution based on a nonlinear elastic medium, *Mechanics of Advanced Materials and Structures,* Vol. 27, No. 20, pp. 1709-1730, 2020.